Title

Oxidation State and Surface Reconstruction of Cu under CO2 Reduction Conditions from In Situ X-ray Characterization

Journal

Journal of the American Chemical Society, 143(2)

ISSN

0002-7863

Authors

Lee, Soo Hong

Lin, John C

Farmand, Maryam

et al.

Publication Date

2021-01-20

DOI

10.1021/jacs.0c10017

JACS
JOURNAL OF THE AMERICAN CHEMICAL SOCIETY
pubs.acs.org/JACS
Communication

Oxidation State and Surface Reconstruction of Cu under CO_2 Reduction Conditions from *In Situ* X-ray Characterization

Soo Hong Lee,[‖] John C. Lin,[‖] Maryam Farmand, Alan T. Landers, Jeremy T. Feaster, Jaime E. Avilés Acosta, Jeffrey W. Beeman, Yifan Ye, Junko Yano, Apurva Mehta,* Ryan C. Davis,* Thomas F. Jaramillo,* Christopher Hahn,* and Walter S. Drisdell*

Cite This: https://dx.doi.org/10.1021/jacs.0c10017
Read Online
ACCESS | Metrics & More | Article Recommendations | Supporting Information

ABSTRACT: The electrochemical CO_2 reduction reaction (CO_2RR) using Cu-based catalysts holds great potential for producing valuable multi-carbon products from renewable energy. However, the chemical and structural state of Cu catalyst surfaces during the CO_2RR remains a matter of debate. Here, we show the structural evolution of the near-surface region of polycrystalline Cu electrodes under *in situ* conditions through a combination of grazing incidence X-ray absorption spectroscopy (GIXAS) and X-ray diffraction (GIXRD). The *in situ* GIXAS reveals that the surface oxide layer is fully reduced to metallic Cu before the onset potential for CO_2RR, and the catalyst maintains the metallic state across the potentials relevant to the CO_2RR. We also find a preferential surface reconstruction of the polycrystalline Cu surface toward (100) facets in the presence of CO_2. Quantitative analysis of the reconstruction profiles reveals that the degree of reconstruction increases with increasingly negative applied potentials, and it persists when the applied potential returns to more positive values. These findings show that the surface of Cu electrocatalysts is dynamic during the CO_2RR, and emphasize the importance of *in situ* characterization to understand the surface structure and its role in electrocatalysis.

Copper is known as the only monometallic heterogeneous electrocatalyst that can convert CO_2 into more valuable multi-carbon products.[1] To produce C_{2+} products at economically feasible reaction rates requires a significant overpotential for CO_2RR.[2] During the CO_2RR, the structure and chemical state of the Cu surface has shown dynamic changes in response to the local environment and applied potential.[3] The Cu valence state at the surface is of particular interest since recent computational studies have shown that the presence of subsurface oxygen or an oxide phase can improve CO_2RR activity and steer the selectivity into C_{2+} products.[4−7] Based on such a hypothesis, several studies have tried to probe the oxidation state of Cu-based catalysts by utilizing *ex situ* and *in situ*/*operando* spectroscopy or microscopy.[8−12] However, these studies have not reached a consensus on whether the oxide phase is present and stable at the catalyst surface under realistic operating conditions where the CO_2RR performance is measured. The rapid reoxidation of the Cu surface upon exposure to O_2 makes it difficult to reach a robust conclusion on this topic, and most of the *in situ*/*operando* techniques employed struggle to distinguish whether the oxygen is located at the surface or buried in the bulk. Therefore, measurements that can specifically probe the active catalytic surface to determine the oxidation states of Cu present under CO_2RR rates similar to those used for performance evaluation are needed.

In addition to the Cu valence state, the surface can dynamically reconstruct through its interaction with the local environment.[13,14] Since Cu has low cohesive energy and high surface mobility, the Cu atoms at the surface can easily migrate. CO, which is a key intermediate in the CO_2RR, has been shown to exacerbate this reconstruction in near-ambient pressure conditions.[15] Surface reconstructions can affect product selectivity because the Cu(111) surface preferentially yields CH_4, whereas the Cu(100) surface produces C_2H_4 with a lower onset potential.[16] To probe the surface structure under CO_2RR conditions, electrochemical scanning tunneling microscopy (ECSTM) has been utilized to image Cu surfaces with atomic resolution and has successfully demonstrated that polycrystalline Cu (hereafter referred to as Cu(pc)) reconstructs into Cu(100) surfaces in N_2-purged electrolytes.[17] However, one of the limitations of ECSTM is its limited field of view, and it is unclear whether these changes occur globally. Therefore, to understand the structural dynamics of Cu surfaces more fully, it is imperative to elucidate both the local atomic structure and long-range order under realistic CO_2RR conditions. Here, we characterize the near-surface structure of a Cu(pc) thin film (50 nm thickness) under CO_2RR conditions by utilizing *in situ* grazing incidence X-ray absorption spectroscopy (GIXAS) and X-ray diffraction (GIXRD). The Cu(pc) thin film is utilized as an electrocatalyst because it has been demonstrated that the roughness of the Cu thin film is low enough to allow sensitivity to a few nm of the

Received: September 18, 2020

https://dx.doi.org/10.1021/jacs.0c10017
J. Am. Chem. Soc. XXXX, XXX, XXX−XXX

surface using GIXAS and GIXRD.[18] We employ an electrochemical flow cell that has been demonstrated to enable near surface-sensitive *in situ* characterization at high current densities by allowing a grazing incidence geometry and improving mass transport of reactive species to the catalyst.[19] Our results confirmed that no detectable oxide remains at the near-surface at potentials relevant to the CO_2RR, and, simultaneously, that potential-dependent surface reconstruction from Cu(pc) to Cu(100) can be observed across μm−mm areas of the surface in a CO_2 saturated electrolyte.

We first characterized as-prepared Cu(pc) films by using GIXRD, GIXAS, and X-ray photoelectron spectroscopy (Figures S1 and S2), and the probe depths were calculated based on the incidence angles (Figure S3). The CO_2RR performance of the Cu(pc) thin film is similar to that of Cu foil reported previously (Figure S4).[20] To investigate the changes of oxidation states and local atomic structure during the CO_2RR, we performed *in situ* GIXAS measurements on the Cu thin film in a 0.1 M $KHCO_3$ electrolyte saturated with CO_2. The total current densities exceeded 20 mA/cm^2 at −1.1 V vs RHE (all the potentials are hereafter noted vs RHE), conditions under which Cu is known to form CO_2RR products and which are often employed when reporting CO_2RR efficiencies (Figure S5). The XANES spectrum at open-circuit potential (OCP) showed rising edge peaks at both 8982 and 8996 eV, indicating that the surface was composed of a mixture of metallic Cu and Cu_2O (Figure 1a). These Cu(I) features disappeared at −0.3 V, which is before the onset potential of CO_2RR on Cu(pc) (generally ∼−0.63 V).[21] Over the applied potential range relevant to the CO_2RR, we observed only metallic Cu at the surface. The corresponding extended X-ray absorption fine structure (EXAFS) spectra displayed a prominent Cu−Cu scattering peak at 2.2 Å, which matches with the metallic Cu reference (Figure 1b). Although angle-dependent overabsorption distorted and dampened XANES and EXAFS spectra,[19] it did not affect the phase information (Figure S6). We obtained similar results in the Ar-purged phosphate and bicarbonate electrolytes, suggesting that the reduction of oxide is primarily driven by the polarization to negative potential (Figure S7). As the GIXAS is highly sensitive to the disordered and local surface structure, our results demonstrate that an oxide phase in the near-surface region was either not present or below our ability to measure.

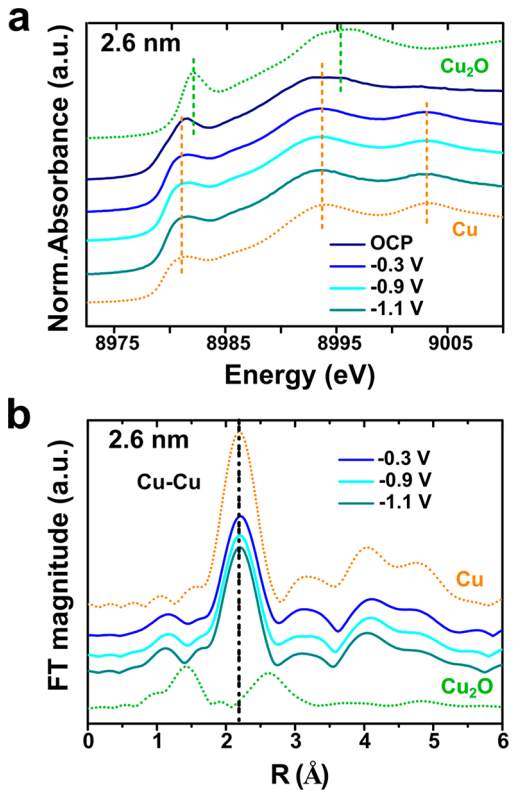

Figure 1. *In situ* GIXAS of Cu(pc) thin-film electrode in CO_2-saturated 0.1 M $KHCO_3$. XANES (a) and EXAFS (b) spectra of Cu (pc) at a probe depth of 2.6 nm as a function of the applied potentials. The Cu (orange) and Cu_2O (green) reference spectra (dotted line) are plotted for comparison.

To elucidate the crystalline structure during CO_2RR, we performed *in situ* GIXRD as a function of probe depth and applied potential in CO_2- and Ar-purged electrolytes (Figure S8). The obtained diffraction measurements were corrected for refraction at the electrode−electrolyte interface (Figure S9a,b) and fit with a pseudo-Voigt function without contribution from electrolytes (Figure S9c). To estimate the uncertainty in determining the Cu(111) peak position, we calculate errors based on the peak asymmetry and sample variations (Figure S10). In the case of the as-synthesized Cu thin film, the *d*-spacing of Cu(111) showed a 0.15% expansion near the surface compared to that of bulk, possibly originating from the existence of the oxide phase (Figure S11). However, at potentials where the CO_2RR occurs, no changes larger than the estimated error in the Cu(111) *d*-spacing values were observed depending on the applied potential and probe depth (Figure S12a). The result with Ar-purged electrolytes is quite similar, except for 0.14% surface expansion at −1.1 V, possibly through hydrogen-induced expansion (Figure S12b).[22] We note that the metallic Cu surface rapidly oxidized into Cu_2O after releasing the applied potential (Figure 2). The Cu_2O phase

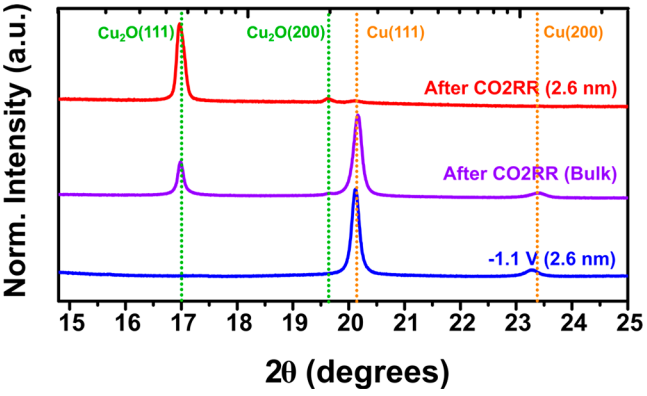

Figure 2. GIXRD of Cu(pc) at a probe depth of 2.6 nm and bulk before and after releasing the applied potential.

was even detected in the bulk within 5 min, demonstrating that the metallic Cu electrode can easily reoxidize at the OCP (generally ∼0.55 V in our case). This result suggests that *ex situ* or *quasi in situ* characterization could contain Cu(I) artifacts on the sample surfaces even without exposure to ambient conditions.

While we observe that the valence state and *d*-spacing of the Cu surface remain unchanged, we do find evidence for surface reconstruction as a function of applied potential. We calculate the area ratio of Cu(200) to Cu(111) Bragg peaks at a probe

https://dx.doi.org/10.1021/jacs.0c10017
J. Am. Chem. Soc. XXXX, XXX, XXX−XXX

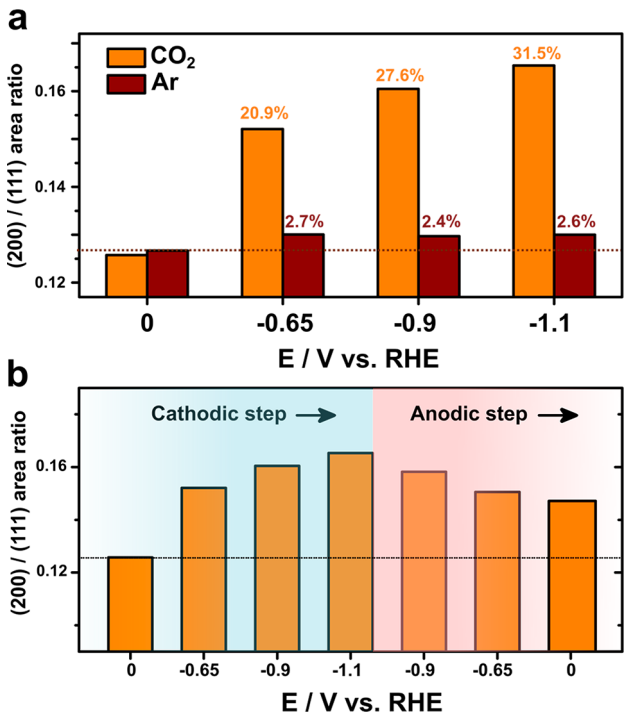

Figure 3. (a) Ratio of the area of Cu(200) to Cu(111) Bragg peaks at a probe depth of 2.6 nm in CO_2- and Ar-purged electrolytes as a function of the applied potentials. Each percentage above the bars indicates an increase of ratio compared to the value at 0 V. The dashed line indicates the ratio in Ar-purged electrolyte at 0 V. (b) Changes of Cu(200)/(111) area ratio at a probe depth of 2.6 nm in cathodic and anodic steps in CO_2-purged electrolyte. The dashed line indicates the ratio at 0 V.

depth of 2.6 nm according to the applied potentials under both CO_2 and Ar-purged electrolytes (Figure 3a). Although peak area is not a rigorously quantitative measure of the amount of specific facet, relative area ratios reflect changes in the preferentially exposed facets on the surface.[23] At 0 V, where no CO_2RR or hydrogen evolution reaction (HER) occurs on Cu(pc), the area ratio in the surface exhibited similar values in CO_2- and Ar-purged electrolytes. As the applied potential becomes more negative, the (200)/(111) area ratio in the surface increases (20.9−31.5%) under CO_2-purged electrolyte, while the area ratio in the Ar-purged electrolyte showed only a slight increase (2.4−2.7%) across the applied potentials. The increase in area ratio was only observed at the probe depth of 2.6 nm, indicating the reconstruction is a surface phenomenon (Figure S13). Both the intensity and integral breadth of the (200)/(111) ratio also increase as a function of the applied potential under CO_2-purged electrolytes (Figure S14). The increase in the area ratio is significantly higher than that of the estimated errors (Figure S15), and the trend is reproduced in another Cu sample (Figure S16). Therefore, these results indicate that a surface reconstruction from Cu(pc) to Cu(100)-like surface occurs during CO_2RR. The differences in CO_2 and Ar-purged electrolytes suggest that surface hydrogen and hydroxide species generated from HER have a limited effect on surface reconstruction. Previous theoretical calculations and spectroscopic observations indicate that the dominant intermediate during CO_2RR is adsorbed CO (CO*).[24,25] We found that the surface reconstruction is enhanced at more negative electrode potentials. Computational results indicate that similar trends in the CO* coverage at these potentials.[26] We also observed a similar reconstruction under CO reduction conditions under alkaline electrolytes in a previous study.[23] Considering that the local pH at the Cu surface increases due to the OH^- ions generated from CO_2RR, we conjecture that the microenvironment under CO_2-purged electrolytes could be similar to the situation under CO-purged alkaline electrolytes. This suggests that CO* is likely a key reaction intermediate in promoting surface reconstruction (see SI for a detailed discussion).

For a more quantitative description of the surface reconstruction, we analyzed the relative changes of the area ratio depending on the applied potential. The area ratio at a probe depth of 2.6 nm increases by 20.9% at −0.65 V compared to the value at 0 V. It is reported that the CO adsorption starts to appear at −0.5 V in a CO_2-saturated 0.1 M $KHCO_3$ electrolyte, and its coverage gradually increases with increasingly negative applied potentials.[25] This accumulated CO* on the surfaces could reconstruct Cu(pc) to Cu(100) before CO_2RR occurs. At −0.9 V, where the C_{2+} products begin to emerge on Cu(pc), the area ratio shows an increase of 27.6% and this change helps to explain why the hydrocarbon formation on Cu(pc) is invariant to that on Cu(100).[27] The area ratio further increases to 31.5% at −1.1 V, where the selectivity toward HER has been reported to surpass the CO_2RR products due to the concentration polarization for CO_2 (i.e., mass transport limitation) in the H-cell configuration.[20] This result implies that enhanced mass transport in our cell allows a higher degree of surface reconstruction to (100) at −1.1 V, possibly through an increase of CO* coverage on the surface. We collected the GIXRD data after reaching a steady state; however, further work is needed to understand the kinetics of surface reconstruction which has been observed on various time scales previously.[17,28] We expect that the high mass transport rates and current densities in our cell translate to fast reconstruction kinetics. We also found that the surface reconstruction is only partially reversible. When the applied potential returns to more positive values, at 0 V the surface displays more (100) faceting than the original surface at 0 V (Figure 3b). The irreversible change of surface morphology has been observed during HER on the Cu(100), leaving behind structural defects such as small holes and clusters.[29] This observation likely explains the previously reported hysteresis of product distribution during cyclic voltammetry.[27,30] In these reports, the enhanced generation of multi-carbon products during cyclic voltammetry has been observed only during the anodic sweep. Our results suggest this may be because the applied potential during the cathodic sweep leads to a significant surface reconstruction to a Cu(100)-like surface that can steer the CO_2RR selectivity toward hydrocarbon formation. During the anodic sweep, the surface is already reconstructed to be more Cu(100)-like, enabling the increased production of C_{2+} products. These results can provide fundamental insights into the previously observed processes that did not take account of the surface reconstruction during CO_2RR.

In summary, we investigated the changes in the valence state and crystallographic structure in the near-surface region of Cu(pc) thin films under realistic CO_2RR conditions. By using an electrochemical flow cell that allows for *in situ* GIXAS and GIXRD with improved CO_2 mass transfer, we successfully demonstrated that the surface copper oxide is reduced to metallic Cu prior to the onset of CO_2RR and that metallic Cu is the only detectable phase during CO_2RR. We also showed

https://dx.doi.org/10.1021/jacs.0c10017
J. Am. Chem. Soc. XXXX, XXX, XXX−XXX

that the surface reconstruction from Cu(pc) to Cu(100) takes place only in the presence of CO_2 molecules, suggesting it is a CO-driven phenomenon. The surface reconstruction increases as the applied potential becomes more negative, and the reconstructed surface partially persists in the anodic steps. Our *in situ* measurements of surface oxidation state and reconstruction behavior provide new insights for the atomic-scale understanding of Cu-based electrocatalysts.

■ ASSOCIATED CONTENT

Supporting Information

The Supporting Information is available free of charge at https://pubs.acs.org/doi/10.1021/jacs.0c10017.

Experimental details, detailed in situ GIXAS and GIXRD supplementary figures, and estimation of error margins (PDF)

Raw data in .txt format for all figures (ZIP)

■ AUTHOR INFORMATION

Corresponding Authors

Apurva Mehta − *Stanford Synchrotron Radiation Lightsource, SLAC National Accelerator Laboratory, Menlo Park, California 94025, United States;* orcid.org/0000-0003-0870-6932; Email: mehta@slac.stanford.edu

Ryan C. Davis − *Stanford Synchrotron Radiation Lightsource, SLAC National Accelerator Laboratory, Menlo Park, California 94025, United States*; Email: rydavis@slac.stanford.edu

Thomas F. Jaramillo − *Department of Chemical Engineering, Stanford University, Stanford, California 94305, United States; SUNCAT Center for Interface Science and Catalysis, SLAC National Accelerator Laboratory, Menlo Park, California 94025, United States;* orcid.org/0000-0001-9900-0622; Email: jaramillo@stanford.edu

Christopher Hahn − *SUNCAT Center for Interface Science and Catalysis, SLAC National Accelerator Laboratory, Menlo Park, California 94025, United States*; Email: chahn@slac.stanford.edu

Walter S. Drisdell − *Joint Center for Artificial Photosynthesis and Chemical Sciences Division, Lawrence Berkeley National Laboratory, Berkeley, California 94720, United States;* orcid.org/0000-0002-8693-4562; Email: wsdrisdell@lbl.gov

Authors

Soo Hong Lee − *Joint Center for Artificial Photosynthesis and Chemical Sciences Division, Lawrence Berkeley National Laboratory, Berkeley, California 94720, United States;* orcid.org/0000-0002-2734-9654

John C. Lin − *Department of Chemical Engineering, Stanford University, Stanford, California 94305, United States; SUNCAT Center for Interface Science and Catalysis, SLAC National Accelerator Laboratory, Menlo Park, California 94025, United States*

Maryam Farmand − *Joint Center for Artificial Photosynthesis and Chemical Sciences Division, Lawrence Berkeley National Laboratory, Berkeley, California 94720, United States*

Alan T. Landers − *SUNCAT Center for Interface Science and Catalysis, SLAC National Accelerator Laboratory, Menlo Park, California 94025, United States; Department of Chemistry, Stanford University, Stanford, California 94305, United States;* orcid.org/0000-0001-7290-711X

Jeremy T. Feaster − *Department of Chemical Engineering, Stanford University, Stanford, California 94305, United States; SUNCAT Center for Interface Science and Catalysis, SLAC National Accelerator Laboratory, Menlo Park, California 94025, United States*

Jaime E. Avilés Acosta − *SUNCAT Center for Interface Science and Catalysis, SLAC National Accelerator Laboratory, Menlo Park, California 94025, United States; Department of Materials Science and Engineering, Stanford University, Stanford, California 94305, United States*

Jeffrey W. Beeman − *Joint Center for Artificial Photosynthesis and Chemical Sciences Division, Lawrence Berkeley National Laboratory, Berkeley, California 94720, United States*

Yifan Ye − *Joint Center for Artificial Photosynthesis, Chemical Sciences Division, and Advanced Light Source, Lawrence Berkeley National Laboratory, Berkeley, California 94720, United States*

Junko Yano − *Joint Center for Artificial Photosynthesis and Molecular Biophysics and Integrated Bioimaging Division, Lawrence Berkeley National Laboratory, Berkeley, California 94720, United States;* orcid.org/0000-0001-6308-9071

Complete contact information is available at: https://pubs.acs.org/10.1021/jacs.0c10017

Author Contributions

‖S.H.L. and J.C.L. contributed equally.

Notes

The authors declare no competing financial interest.

■ ACKNOWLEDGMENTS

The material for synthesis of Cu thin films, electrochemical flow cell assembly, and GIXAS and GIXRD measurements is based on work performed by the Joint Center for Artificial Photosynthesis, a DOE Energy Innovation Hub, supported through the Office of Science of the U.S. Department of Energy, under Award No. DE-SC0004993. The material for electrochemistry experiments with product analysis is based on work performed by the Liquid Sunlight Alliance, which is supported by the U.S. Department of Energy, Office of Science, Office of Basic Energy Sciences, Fuels from Sunlight Hub under Award No. DE-SC0021266. Use of the Stanford Synchrotron Radiation Lightsource, SLAC National Accelerator Laboratory, is supported by the U.S. Department of Energy, Office of Science, Office of Basic Energy Sciences under Contract No. DE-AC02-76SF00515. Part of this work was performed at the Stanford Nano Shared Facilities (SNSF) and the Stanford Nanofabrication Facility (SNF), supported by the National Science Foundation under Award ECCS-1542152.

■ REFERENCES

(1) Nitopi, S.; Bertheussen, E.; Scott, S. B.; Liu, X.; Engstfeld, A. K.; Horch, S.; Seger, B.; Stephens, I. E. L.; Chan, K.; Hahn, C.; Nørskov, J. K.; Jaramillo, T. F.; Chorkendorff, I. Progress and Perspectives of Electrochemical CO_2 Reduction on Copper in Aqueous Electrolyte. *Chem. Rev.* **2019**, *119* (12), 7610−7672.

(2) Peterson, A. A.; Abild-Pedersen, F.; Studt, F.; Rossmeisl, J.; Nørskov, J. K. How copper catalyzes the electroreduction of carbon dioxide into hydrocarbon fuels. *Energy Environ. Sci.* **2010**, *3* (9), 1311−1315.

(3) Handoko, A. D.; Wei, F.; Jenndy; Yeo, B. S.; Seh, Z. W. Understanding heterogeneous electrocatalytic carbon dioxide reduc-

https://dx.doi.org/10.1021/jacs.0c10017
J. Am. Chem. Soc. XXXX, XXX, XXX−XXX

tion through operando techniques. *Nat. Catal.* **2018**, *1* (12), 922−934.
(4) Xiao, H.; Goddard, W. A.; Cheng, T.; Liu, Y. Cu metal embedded in oxidized matrix catalyst to promote CO_2 activation and CO dimerization for electrochemical reduction of CO_2. *Proc. Natl. Acad. Sci. U. S. A.* **2017**, *114* (26), 6685−6688.
(5) De Luna, P.; Quintero-Bermudez, R.; Dinh, C.-T.; Ross, M. B.; Bushuyev, O. S.; Todorović, P.; Regier, T.; Kelley, S. O.; Yang, P.; Sargent, E. H. Catalyst electro-redeposition controls morphology and oxidation state for selective carbon dioxide reduction. *Nat. Catal.* **2018**, *1* (2), 103−110.
(6) Liu, C.; Lourenço, M. P.; Hedström, S.; Cavalca, F.; Diaz-Morales, O.; Duarte, H. A.; Nilsson, A.; Pettersson, L. G. M. Stability and Effects of Subsurface Oxygen in Oxide-Derived Cu Catalyst for CO_2 Reduction. *J. Phys. Chem. C* **2017**, *121* (45), 25010−25017.
(7) Favaro, M.; Xiao, H.; Cheng, T.; Goddard, W. A.; Yano, J.; Crumlin, E. J. Subsurface oxide plays a critical role in CO_2 activation by Cu(111) surfaces to form chemisorbed CO_2, the first step in reduction of CO_2. *Proc. Natl. Acad. Sci. U. S. A.* **2017**, *114* (26), 6706−6711.
(8) Zhao, Y.; Chang, X.; Malkani, A. S.; Yang, X.; Thompson, L.; Jiao, F.; Xu, B. Speciation of Cu Surfaces During the Electrochemical CO Reduction Reaction. *J. Am. Chem. Soc.* **2020**, *142* (21), 9735−9743.
(9) Firet, N. J.; Burdyny, T.; Nesbitt, N. T.; Chandrashekar, S.; Longo, A.; Smith, W. A. Copper and silver gas diffusion electrodes performing CO_2 reduction studied through operando X-ray absorption spectroscopy. *Catal. Sci. Technol.* **2020**, *10* (17), 5870−5885.
(10) Mistry, H.; Varela, A. S.; Bonifacio, C. S.; Zegkinoglou, I.; Sinev, I.; Choi, Y.-W.; Kisslinger, K.; Stach, E. A.; Yang, J. C.; Strasser, P.; Cuenya, B. R. Highly selective plasma-activated copper catalysts for carbon dioxide reduction to ethylene. *Nat. Commun.* **2016**, *7* (1), 12123.
(11) Cavalca, F.; Ferragut, R.; Aghion, S.; Eilert, A.; Diaz-Morales, O.; Liu, C.; Koh, A. L.; Hansen, T. W.; Pettersson, L. G. M.; Nilsson, A. Nature and Distribution of Stable Subsurface Oxygen in Copper Electrodes During Electrochemical CO_2 Reduction. *J. Phys. Chem. C* **2017**, *121* (45), 25003−25009.
(12) Velasco-Velez, J.-J.; Mom, R. V.; Sandoval-Diaz, L.-E.; Falling, L. J.; Chuang, C.-H.; Gao, D.; Jones, T. E.; Zhu, Q.; Arrigo, R.; Roldan Cuenya, B.; Knop-Gericke, A.; Lunkenbein, T.; Schlögl, R. Revealing the Active Phase of Copper during the Electroreduction of CO_2 in Aqueous Electrolyte by Correlating *In Situ* X-ray Spectroscopy and *In Situ* Electron Microscopy. *ACS Energy Lett.* **2020**, *5* (6), 2106−2111.
(13) Kondrat, S. A.; van Bokhoven, J. A. A Perspective on Counting Catalytic Active Sites and Rates of Reaction Using X-Ray Spectroscopy. *Top. Catal.* **2019**, *62* (17), 1218−1227.
(14) Huang, J.; Hörmann, N.; Oveisi, E.; Loiudice, A.; De Gregorio, G. L.; Andreussi, O.; Marzari, N.; Buonsanti, R. Potential-induced nanoclustering of metallic catalysts during electrochemical CO_2 reduction. *Nat. Commun.* **2018**, *9* (1), 3117.
(15) Eren, B.; Zherebetskyy, D.; Patera, L. L.; Wu, C. H.; Bluhm, H.; Africh, C.; Wang, L.-W.; Somorjai, G. A.; Salmeron, M. Activation of Cu(111) surface by decomposition into nanoclusters driven by CO adsorption. *Science* **2016**, *351* (6272), 475−478.
(16) Hori, Y.; Wakebe, H.; Tsukamoto, T.; Koga, O. Adsorption of CO Accompanied with Simultaneous Charge Transfer on Copper Single Crystal Electrodes Related with Electrochemical Reduction of CO_2 to hydrocarbons. *Surf. Sci.* **1995**, *335*, 258−263.
(17) Kim, Y.-G.; Baricuatro, J. H.; Soriaga, M. P. Surface Reconstruction of Polycrystalline Cu Electrodes in Aqueous $KHCO_3$ Electrolyte at Potentials in the Early Stages of CO_2 Reduction. *Electrocatalysis* **2018**, *9* (4), 526−530.
(18) Hahn, C.; Hatsukade, T.; Kim, Y.-G.; Vailionis, A.; Baricuatro, J. H.; Higgins, D. C.; Nitopi, S. A.; Soriaga, M. P.; Jaramillo, T. F. Engineering Cu surfaces for the electrocatalytic conversion of CO_2: Controlling selectivity toward oxygenates and hydrocarbons. *Proc. Natl. Acad. Sci. U. S. A.* **2017**, *114* (23), 5918−5923.
(19) Farmand, M.; Landers, A. T.; Lin, J. C.; Feaster, J. T.; Beeman, J. W.; Ye, Y.; Clark, E. L.; Higgins, D.; Yano, J.; Davis, R. C.; Mehta, A.; Jaramillo, T. F.; Hahn, C.; Drisdell, W. S. Electrochemical flow cell enabling operando probing of electrocatalyst surfaces by X-ray spectroscopy and diffraction. *Phys. Chem. Chem. Phys.* **2019**, *21* (10), 5402−5408.
(20) Clark, E. L.; Resasco, J.; Landers, A.; Lin, J.; Chung, L.-T.; Walton, A.; Hahn, C.; Jaramillo, T. F.; Bell, A. T. Standards and Protocols for Data Acquisition and Reporting for Studies of the Electrochemical Reduction of Carbon Dioxide. *ACS Catal.* **2018**, *8* (7), 6560−6570.
(21) Kuhl, K. P.; Cave, E. R.; Abram, D. N.; Jaramillo, T. F. New Insights into the Electrochemical Reduction of Carbon Dioxide on Metallic Copper Surfaces. *Energy Environ. Sci.* **2012**, *5*, 7050−7059.
(22) Huynh, T. M. T.; Broekmann, P. From In Situ towards In Operando Conditions: Scanning Tunneling Microscopy Study of Hydrogen Intercalation in Cu(111) during Hydrogen Evolution. *ChemElectroChem* **2014**, *1* (8), 1271−1274.
(23) Scott, S. B.; Hogg, T. V.; Landers, A. T.; Maagaard, T.; Bertheussen, E.; Lin, J. C.; Davis, R. C.; Beeman, J. W.; Higgins, D.; Drisdell, W. S.; Hahn, C.; Mehta, A.; Seger, B.; Jaramillo, T. F.; Chorkendorff, I. Absence of Oxidized Phases in Cu under CO Reduction Conditions. *ACS Energy Lett.* **2019**, *4* (3), 803−804.
(24) Tang, M. T.; Ulissi, Z. W.; Chan, K. Theoretical Investigations of Transition Metal Surface Energies under Lattice Strain and CO Environment. *J. Phys. Chem. C* **2018**, *122* (26), 14481−14487.
(25) Zhu, S.; Jiang, B.; Cai, W.-B.; Shao, M. Direct Observation on Reaction Intermediates and the Role of Bicarbonate Anions in CO_2 Electrochemical Reduction Reaction on Cu Surfaces. *J. Am. Chem. Soc.* **2017**, *139* (44), 15664−15667.
(26) Luo, W.; Nie, X.; Janik, M. J.; Asthagiri, A. Facet Dependence of CO_2 Reduction Paths on Cu Electrodes. *ACS Catal.* **2016**, *6* (1), 219−229.
(27) Schouten, K. J. P.; Qin, Z.; Pérez Gallent, E.; Koper, M. T. M. Two Pathways for the Formation of Ethylene in CO Reduction on Single-Crystal Copper Electrodes. *J. Am. Chem. Soc.* **2012**, *134* (24), 9864−9867.
(28) Gunathunge, C. M.; Li, X.; Li, J.; Hicks, R. P.; Ovalle, V. J.; Waegele, M. M. Spectroscopic Observation of Reversible Surface Reconstruction of Copper Electrodes under CO_2 Reduction. *J. Phys. Chem. C* **2017**, *121* (22), 12337−12344.
(29) Matsushima, H.; Taranovskyy, A.; Haak, C.; Gründer, Y.; Magnussen, O. M. Reconstruction of Cu(100) Electrode Surfaces during Hydrogen Evolution. *J. Am. Chem. Soc.* **2009**, *131* (30), 10362−10363.
(30) Clark, E. L.; Bell, A. T. Direct Observation of the Local Reaction Environment during the Electrochemical Reduction of CO_2. *J. Am. Chem. Soc.* **2018**, *140* (22), 7012−7020.

https://dx.doi.org/10.1021/jacs.0c10017
J. Am. Chem. Soc. XXXX, XXX, XXX−XXX